iJRASET
International Journal For Research in Applied Science and Engineering Technology

# INTERNATIONAL JOURNAL FOR RESEARCH

IN APPLIED SCIENCE & ENGINEERING TECHNOLOGY

**Volume:** 7 **Issue:** VII **Month of publication:** July 2019

**DOI:** http://doi.org/10.22214/ijraset.2019.7031

www.ijraset.com

Call: 08813907089 | E-mail ID: ijraset@gmail.com

International Journal for Research in Applied Science & Engineering Technology (IJRASET)
*ISSN: 2321-9653; IC Value: 45.98; SJ Impact Factor: 7.177*
*Volume 7 Issue VII, July 2019- Available at www.ijraset.com*

# Free Vibration Analysis of FG-GNP Reinforced Composite Plates using Higher Order Shear Deformation Theory

SR sampoorna[1], J. Sureh Kumar[2]
[1]*P.G Student,* [2]*Professor, Department of Mechanical Engineering, JNTUH College of Engineering, Kukatpally, Hyderabad, India*

***Abstract***: ***The major objective of the present study is to determine the vibrational characteristics of simply supported functionally graded GNP reinforced composite plates with various graphene nano platelets (GNP) distributions, weight fractions of GNP, length-to-thickness ratio through-the-thickness by means of a higher order displacement model. The equations of motion for the present model are derived using the Hamilton's principle. The vibration characteristics of the model in the closed form are obtained by using Navier's method under simply supported boundary conditions. The fundamental frequency of FG-GNP reinforced composite rectangular plate under the given boundary conditions are presented for different aspect ratios. The present results are compared with the solutions of the other FSDTs available in the literature. It can be concluded that the proposed theory is accurate and efficient in estimating the vibration characteristics of FG-GNP plates.***
***Keywords: Vibrational characteristics, FG-GNP plates, effective material properties, HSDT, Hamilton's principle, Navier's Method.***

## I. INTRODUCTION

Functionally graded materials (FGMs) are new type of composites involving continuously varying micro structure, which lead to variation of physical and mechanical properties through the thickness. Because of these features application of functionally graded materials (FGM) has increased in present days. These materials are advanced, heat resisting, erosion and corrosion resistant and components made of FG materials can be used in many engineering fields such as aero space, mechanical, nuclear energy, chemical plant, electronics and bio medical applications. Graphene is an effective reinforcement material in the case of composite material for the variety of applications. Graphene is an amazingly pure substance with simple and orderly structure based on tight, regular, atomic bonding, which is carbon based material in fact it behaves much more like a metal(though the way it conducts electricity is different) because of this some scientists describe it as semi metal or a semiconductor. Graphene filled polymer or ceramic matrix Functional graded composites exhibit continuous improvements in properties such as thermo mechanical, chemical, light in weight, dimensional stability, heat and corrosion resistance and electrical conductivity. By the concept of functionally graded (FG) materials, a new type of FG-graphene nano platelets (GNP) reinforced composite, has been proposed making use of graphene as the reinforcements in a functionally graded composite and the fabrication process is powder metallurgy. Graphene reinforced composites derived with a non-uniform distribution of graphene through the matrix material. The present work deals with the analytical formulations and solutions for the vibration analysis of FG-GNP reinforced composite plates using higher order shear deformation theory (HSDT) without enforcing zero transverse shear stress on the top and bottom surfaces of the plate. The theoretical model presented which incorporates the transverse extensibility which accounts for the transverse effects. Thus a shear correction factor is not needed. The plate material properties will be changing through the thickness direction. The governing equations and boundary conditions for plate are derived by using the principle of virtual work also called as Hamilton's Principle. Solutions are obtained for FG-GNP reinforced composite plates in closed-form using Navier's technique and solving the Eigen value equation.

## II. THEORETICAL FORMULATION AND DEVELOPMENT OF HIGHER ORDER THEORY

The thick FG-graphene reinforced composite plate shown in Fig. 1 is studied in this investigation. The plate is subjected to transverse loads. The length, width and thickness of the FG-graphene reinforced composite plate are a, b and h respectively. $N_x$ and $N_y$ define the in-plane loads along the x and y directions, respectively. Two types of distributions for the graphene in the FG-graphene reinforced composite plates are studied, and these graphene configurations are displayed in Fig. 2, where the uniform distribution and the other graphene distribution are denoted by UD and FGX respectively. In FGX, the top and bottom surfaces of the plate is graphene-rich. The effective youngs modulus is

$$E_C = \frac{3}{8}E_{\parallel} + \frac{5}{8}E_{\perp} \quad \text{..... (2.a)}$$

Where Longitudinal modulus $E_{\parallel}$ and Transverse modulus $E_{\perp}$ can be determined by Halpin-Tsai model

$$E_{\parallel} = \frac{1+\xi_L \eta_L V_{GNP}}{1-\eta_L V_{GNP}} \times E_M \quad \text{..... (2.b)}$$

$$E_{\perp} = \frac{1+\xi_W \eta_W V_{GNP}}{1-\eta_W V_{GNP}} \times E_M \quad \text{..... (2.c)}$$

Where

$$\eta_L = \frac{\frac{E_{GNP}}{E_M} - 1}{\frac{E_{GNP}}{E_M} + \xi_L} \quad \text{.....(2.d)}$$

$$\eta_W = \frac{\frac{E_{GNP}}{E_M} - 1}{\frac{E_{GNP}}{E_M} + \xi_W} \quad \text{.....(2.e)}$$

$E_M$ and $E_{GNP}$ are young's moduli of polymer matrix and graphene platelets (GNPs) respectively, $V_{GNP}$ is GNP volume fraction, $\xi_L$ and $\xi_W$ are the parameters characterizing both the geometry and size of GNP nano platelets , defined as

$$\xi_L = 2\left(\frac{l_{GNP}}{h_{GNP}}\right) \quad \text{.....(2.f)}$$

$$\xi_W = 2\left(\frac{w_{GNP}}{h_{GNP}}\right) \quad \text{.....(2.g)}$$

In which $l_{GNP}$ , $w_{GNP}$ and $h_{GNP}$ are the average length , width, and thickness of the GNPs respectively. Mass density $\rho_c$ and poission's ratio $\upsilon_c$ of the GPN / polymer nano composite can be calculated by rule of mixture (ROM).

$$\rho_c = \rho_{GNP} V_{GNP} + \rho_M V_M \quad \text{..... (2.h)}$$

$$\upsilon_c = \upsilon_{GNP} V_{GNP} + \upsilon_M V_M \quad \text{..... (2.i)}$$

Where $V_M$ is the volume fraction of polymer matrix, $V_{GNP}$ is volume fraction of GNP is calculated by given formula

$$V_{GNP} = \frac{g_{GNP}}{g_{GNP} + (\rho^{GNP}/\rho^{m})(1-g_{GNP})} \quad \text{..... (2.j)}$$

in which $g_{GNP}$ is the fraction of weight of the graphene, and $\rho^{m}$ and $\rho^{GNP}$ are densities of the matrix and graphene nano platelets. $V_{GNP}$ $and$ $V_m$ are the volume fractions of the graphene and matrix, and their sum must be equal to 1, that is $V_{GNP} + V_m = 1$.

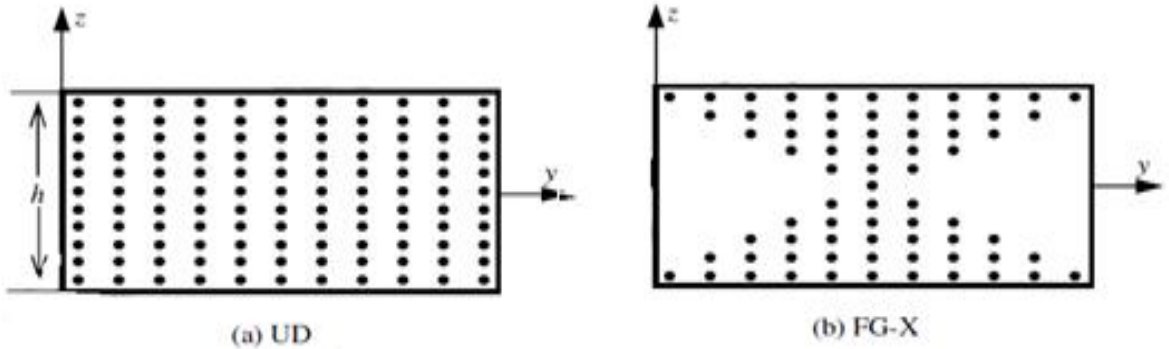


Figure 1 Schematic diagram of the two distributions of graphene.

*ISSN: 2321-9653; IC Value: 45.98; SJ Impact Factor: 7.177*
*Volume 7 Issue VII, July 2019- Available at www.ijraset.com*

The weight fractions of the two distribution types expressed as:

$g_{GNP}(z) = g_{GNP}$ ,(UD) .....(2.k)

$g_{GNP}(z) = 4g_{GNP}(0.5 + |K - (N_L + 1)/2|)/(2 + N_L)$ , (FGX) .....(2.l)

*A. Displacement Model*

In formulating the higher-order shear deformation theory, a plate of $0 \le x \le a\,;\, 0 \le y \le b$ and $-\frac{h}{2} \le z \le \frac{h}{2}$ is considered as shown in figure.2

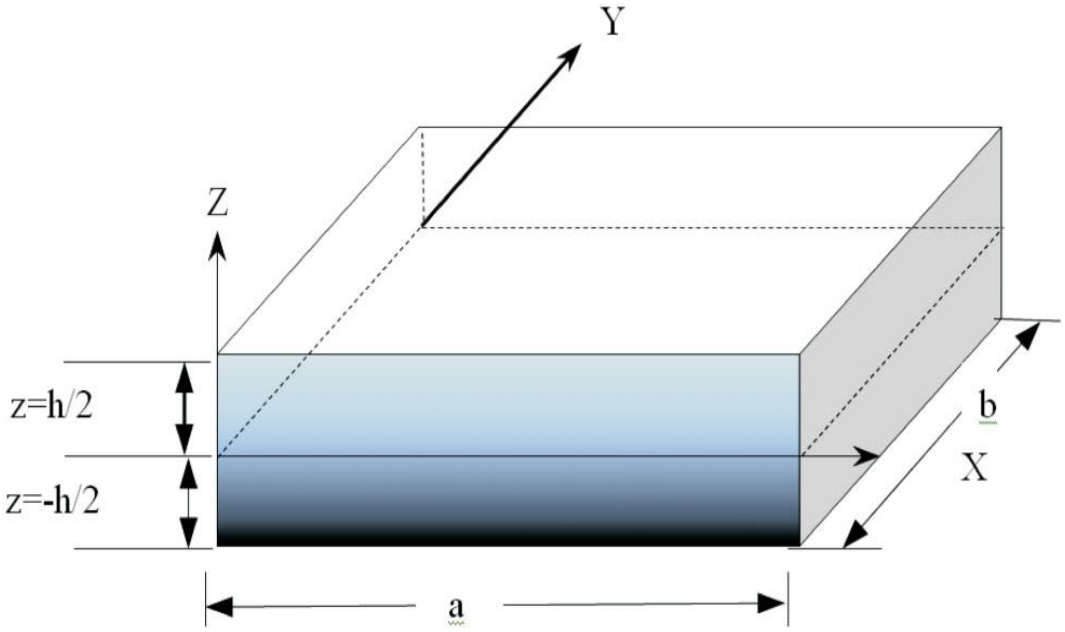


Fig.2 Functionally graded plate with coordinates.

In order to approximate 3D-elasticity plate problem to 2D one, the displacement components u (x, y, z), v (x, y, z) and w (x, y, z) at any point in the plate are expanded in terms of the thickness coordinate. The elasticity solution indicates that the transverse shear stress varies parabolically through the plate thickness. This requires the use of a displacement field, in which the in-plane displacements are expanded as cubic functions of the thickness coordinate. The displacement field which assumes w (x, y, z) constant through the plate thickness thus setting $\varepsilon_z = 0$ is expressed as:

$$\left.\begin{aligned} u(x,y,z) &= u_o(x,y) + z\theta_x(x,y) + z^2 u_o^*(x,y) + z^3\theta_x^*(x,y) \\ v(x,y,z) &= v_o(x,y) + z\theta_y(x,y) + z^2 v_o^*(x,y) + z^3\theta_y^*(x,y) \\ w(x,y,z) &= w_o(x,y) \end{aligned}\right\} \quad \text{..... (2.1)}$$

Where the parameters $u_0$, $v_0$, $w_0$ denote the displacements of a point (x, y) on the mid-plane. The functions $\theta_x$, $\theta_y$ are rotations of the normal to the mid-plane about y and x axes, respectively. The parameters $u_0^*$, $v_o^*$, $\theta_x^*$, $\theta_y^*$ are the corresponding higher-order deformation terms.

In present work, analytical formulation and solution were obtained without enforcing zero transverse shear stress conditions on the top and bottom surfaces of the plate. In formulating the theory, the following assumptions are considered:

*1)* The layers are perfectly bonded together.
*2)* The material of each layer is linearly elastic and has three planes of material symmetry (i.e., Orthotropic).
*3)* Each layer is of uniform thickness.
*4)* The strains and displacements are small.

*B. Strain- displacement Relations:*

The higher-order theories introduce additional unknowns that are often difficult to interpret in physical terms. The third order laminate theory with transverse inextensibility based on the displacement field is shown in Eq. (2.1).

By substitution of the displacement relations in Eq. (2.3) in to strain displacement equations of the classical theory of elasticity the following relations are obtained:

$$\varepsilon_x = \varepsilon_{xo} + zk_x + z^2\varepsilon^*_{xo} + z^3k^*_x$$
$$\varepsilon_y = \varepsilon_{yo} + zk_y + z^2\varepsilon^*_{yo} + z^3k^*_y$$
$$\varepsilon_z = 0$$
$$\gamma_{xy} = \varepsilon_{xyo} + zk_{xy} + z^2\varepsilon^*_{xyo} + z^3k^*_{xy} \quad \text{.....(2.2.a)}$$
$$\gamma_{yz} = \phi_y + z\varepsilon_{yzo} + z^2\phi^*_y$$
$$\gamma_{xz} = \phi_x + z\varepsilon_{xzo} + z^2\phi^*_x$$

where,

$$\varepsilon_{xo} = \frac{\partial uo}{\partial x},\ \varepsilon_{yo} = \frac{\partial vo}{\partial y},\ \varepsilon_{xyo} = \frac{\partial uo}{\partial y} + \frac{\partial v_o}{\partial x}$$
$$k_x = \frac{\partial \theta_x}{\partial x},\ k_y = \frac{\partial \theta_y}{\partial y},\ k_{xy} = \frac{\partial \theta_x}{\partial y} + \frac{\partial \theta_y}{\partial x}$$
$$k^*_x = \frac{\partial \theta^*_x}{\partial x},\ k^*_y = \frac{\partial \theta^*_y}{\partial y},\ k^*_{xy} = \frac{\partial \theta^*_x}{\partial y} + \frac{\partial \theta^*_y}{\partial x}$$
$$\varepsilon^*_{xo} = \frac{\partial u^*_o}{\partial x},\ \varepsilon^*_{yo} = \frac{\partial v^*_o}{\partial y}, \varepsilon^*_{xyo} = \frac{\partial u^*_o}{\partial y} + \frac{\partial v^*_o}{\partial x},$$
$$\phi_y = \theta_y + \frac{\partial w_o}{\partial y},\ \phi_x = \theta_x + \frac{\partial w_o}{\partial x}, \quad \text{.....(2.2.b)}$$
$$\varepsilon_{yzo} = 2v^*_o, \varepsilon_{xzo} = 2u^*_o,\ \phi^*_y = 3\theta^*_y,\ \phi^*_x = 3\theta^*_x$$

*C. Constitutive Relations*

Since $\varepsilon_z = 0$, the transverse normal stress $\sigma_z$, although not zero identically, does not appear in the virtual work statement and hence in the equations of motion. Consequently, it amounts to neglecting the transverse normal stress. Thus we have, in theory, a case of plane stress. For an FG-graphene reinforced composite laminate, the plane stress reduced elastic constants and the transformed plane stress reduced elastic constants will be same i.e., $C_{ij} = Q_{ij}$. The linear constitutive relations for the plate in the given coordinates (x-y-z) are:

$$\begin{Bmatrix}\sigma_x\\ \sigma_y\\ \tau_{xy}\end{Bmatrix}^L = \begin{bmatrix}Q_{11} & Q_{12} & 0\\ Q_{12} & Q_{22} & 0\\ 0 & 0 & Q_{33}\end{bmatrix}^L \begin{Bmatrix}\varepsilon_x\\ \varepsilon_y\\ \gamma_{xy}\end{Bmatrix}^L \quad \text{.....(2.3.a)}$$
$$\begin{Bmatrix}\tau_{yz}\\ \tau_{xz}\end{Bmatrix}^L = \begin{bmatrix}Q_{44} & 0\\ 0 & Q_{55}\end{bmatrix}^L \begin{Bmatrix}\gamma_{yz}\\ \gamma_{xz}\end{Bmatrix}^L$$

$\sigma_x, \sigma_y, \tau_{xy}, \tau_{yz}, \tau_{xz}$ are the stresses and $\varepsilon_x, \varepsilon_y, \gamma_{xy}, \gamma_{yz}, \gamma_{xz}$ are the linear strains with respect to the laminate axes.

$Q_{ij}$ are the transformed plane stress reduced elastic constants in the plate axes of the Lth lamina.

$$Q_{11} = \frac{E_C}{(1-\upsilon_{12}\upsilon_{21})}, \quad Q_{22} = \frac{E_C}{(1-\upsilon_{12}\upsilon_{21})}, \quad Q_{12} = \frac{\upsilon_{21}E_C}{(1-\upsilon_{12}\upsilon_{21})},$$
$$Q_{33} = G_{12}, Q_{44} = G_{23}, Q_{55} = G_{13}$$

where,

$E_c$ = Young's modulus of elasticity in the i direction.

$\upsilon_{ij}$ = Poisson's ratios that give strain in the j direction due to stress in the i direction.

$G_{ij}$ =shear moduli

*D. Equations of motion:*

The work done by actual forces in moving through virtual displacements, that are consistent with the geometric constraints of a body is set to zero to obtain the equations of motion and this is known as energy principle. It is useful in deriving governing equations, boundary conditions and obtaining approximate solutions by virtual methods. For simple mechanical systems, for which the free body diagram is set up, the vector approach provides an easy and direct way of deriving governing equations. However, for complicated systems the procedure becomes more cumbersome and intractable. In such cases, energy principles provide alternative means to obtain the governing equations and their solutions. In the present study, the principle of virtual work is used to derive the equations of motion of laminated plates.

The governing equations of higher-order theory for Eq. (2.1) will be derived using the dynamic version of the principle of virtual displacements, i.e.

$$\int_0^T (\delta U + \delta V - \delta K)\, dt = 0 \qquad \text{.....(2.4.a)}$$

Where,

δU = Virtual strain energy

δV = Virtual work done by applied forces

δK = Virtual kinetic energy

δU+δV=total potential energy

The virtual strain energy, work done and kinetic energy are given by

$$\delta U = \int_A \left\{ \int_{-h/2}^{h/2} \left[\sigma_x \delta\varepsilon_x + \sigma_y \delta\varepsilon_y + \tau_{xy}\delta\gamma_{xy} + \tau_{xz}\delta\gamma_{xz} + \tau_{yz}\delta\gamma_{yz}\right] dz \right\} dx\, dy$$

$\delta V = -\int q\delta w_0 \, dx \, dy$

$$\delta K = \int_A \{ \int_{-h/2}^{h/2} \rho_0 \left[ \left(\dot{u}_0 + Z\dot{\theta}_x + Z^2 \dot{u}_0^* + Z^3 \dot{\theta}_x^*\right)\left(\delta\dot{u}_0 + Z\delta\dot{\theta}_x + Z^2 \delta\dot{u}_0^* + Z^3 \delta\dot{\theta}_x^*\right) + \left(\dot{v}_0 + Z\dot{\theta}_y + Z^2 \dot{v}_0^* + Z^3 \dot{\theta}_y^*\right)\left(\delta\dot{v}_0 + Z\delta\dot{\theta}_y + Z^2\delta \dot{v}_0^* + Z^3\delta \dot{\theta}_y^*\right) + \dot{w}_0\delta\dot{w}_0 \right] dz \} dx\, dy$$

…….(2.4.b).

Where,

q = distributed load over the surface of the plate.

$\rho_0$ = Density of plate material

*ISSN: 2321-9653; IC Value: 45.98; SJ Impact Factor: 7.177*
*Volume 7 Issue VII, July 2019- Available at www.ijraset.com*

$\dot{u}_0 = \partial u_0 / \partial t$, $\dot{v}_0 = \partial v_0 / \partial t$ etc. indicates the time derivatives

On substituting for δU, δV and δK from Eq. (2.4.b) in to the virtual work statement in Eq. (2.4.a) and integrating through the thickness of the plate, rewriting it in matrix form and the stess strain relations of plate given by;

$$\begin{Bmatrix} N_x & | & N_x^* \\ N_y & | & N_y^* \\ N_{xy} & | & N_{xy}^* \end{Bmatrix} = \sum_{L=1}^{n} \int_{h_{L-1}}^{h_L} \begin{Bmatrix} \sigma_x \\ \sigma_y \\ \tau_{xy} \end{Bmatrix} \begin{bmatrix} 1 & | & z^2 \end{bmatrix} dz$$

$$\begin{Bmatrix} M_x & | & M_x^* \\ M_y & | & M_y^* \\ M_{xy} & | & M_{xy}^* \end{Bmatrix} = \sum_{L=1}^{n} \int_{h_{L-1}}^{h_L} \begin{Bmatrix} \sigma_x \\ \sigma_y \\ \tau_{xy} \end{Bmatrix} \begin{bmatrix} Z & | & Z^3 \end{bmatrix} dz \qquad \text{……(2.4.c)}$$

Transverse force resultants and the inertias are given by:

$$\begin{Bmatrix} Q_x & | & S_x & | & Q_x^* \\ Q_y & | & S_y & | & Q_y^* \end{Bmatrix} = \sum_{L=1}^{n} \int_{h_{L-1}}^{h_L} \begin{Bmatrix} \tau_{xz} \\ \tau_{yz} \end{Bmatrix} \begin{bmatrix} 1 & | & Z & | & Z^2 \end{bmatrix} dz \qquad \text{……(2.4.d)}$$

$$.. I_1, I_2, I_3, I_4, I_5, I_6, I_7 = \int_{-h/2}^{h/2} \rho_0 (1, z, z^2, z^3, z^4, z^5, z^6)\, dz \qquad \text{…….(2.4.e)}$$

By substituting Eq. (2.3.a) into Eq. (2.4.f), upon integration these expressions are rewritten in a matrix form which defines the stress/strain relations of the laminate are given by:

$$\begin{Bmatrix} N \\ N^* \\ -- \\ M \\ M^* \\ -- \\ Q \\ Q^* \end{Bmatrix} = \begin{bmatrix} \overline{A} & | & \overline{B} & | & \overline{0} \\ \overline{B^t} & | & \overline{D_b} & | & \overline{0} \\ \overline{0} & | & \overline{0} & | & \overline{D_s} \end{bmatrix} \begin{Bmatrix} \varepsilon_0 \\ \varepsilon_0^* \\ -- \\ K \\ K^* \\ -- \\ \phi \\ \phi^* \end{Bmatrix} \qquad \text{…….(2.4.f)}$$

Where,

$N = [N_x \quad N_y \quad N_{xy}]^t$ ; $N^* = [N_x^* \quad N_y^* \quad N_{xy}^*]^t$

N, $N^*$ are called the in-plane force resultants

$M = [M_x \quad M_y \quad M_{xy}]^t$ ; $M^* = [M_x^* \quad M_y^* \quad M_{xy}^*]^t$

M, $M^*$ are called as moment resultants

$Q = [Q_x \quad Q_y]^t$ ; $Q^* = [S_x \quad S_y \quad Q_x^* \quad Q_y^*]^t$

Q, $Q^*$ denotes the transverse force resultants and also

$$\varepsilon_0 = [\varepsilon_{x0} \ \varepsilon_{y0} \ \varepsilon_{xy0}]^t \ ; \varepsilon_0^* = [\varepsilon_{x0}^* \ \varepsilon_{y0}^* \ \varepsilon_{xy0}^*]^t$$

$$k = [k_x \ k_y \ k_{xy}]^t \ ; k^* = [k_x^* \ k_y^* \ k_{xy}^*]^t$$

$$\phi = [\phi_x \ \phi_y]^t ; \phi^* = [\varepsilon_{xz0} \ \varepsilon_{yz0} \ \phi_x^* \ \phi_y^*]^t$$

Integrating the resulting above Equations by parts and collecting coefficients of each of virtual displacements $\delta u_o \delta v_0$, $\delta w_0$, $\delta\theta_x$, $\delta\theta_y$, $\delta u_0^*$, $\delta v_0^*$, $\delta\theta_x^*$, $\delta\theta_y^*$ together and virtual displacements are zero, the following equations of motion are obtained as:

$$\delta u_0 : \frac{\partial N_x}{\partial x} + \frac{\partial N_{xy}}{\partial y} = I_1 \ddot{u}_0 + I_2(\ddot{\theta}_x) + I_3 \ddot{u}_0^* + I_4 \ddot{\theta}_x^*$$

$$\delta v_0 : \frac{\partial N_y}{\partial y} + \frac{\partial N_{xy}}{\partial x} = I_1 \ddot{v}_0 + I_2(\ddot{\theta}_y) + I_3 \ddot{v}_0^* + I_4 \ddot{\theta}_y^*$$

$$\delta w_0 : \frac{\partial Q_x}{\partial x} + \frac{\partial Q_y}{\partial y} + q = I_1 \ddot{w}_0$$

$$\delta\theta_x : \frac{\partial M_x}{\partial x} + \frac{\partial M_{xy}}{\partial y} - Q_x = I_2 \ddot{u}_0 + I_3(\ddot{\theta}_x) + I_4 \ddot{u}_0^* + I_5 \ddot{\theta}_x^*$$

$$\delta\theta_y : \frac{\partial M_y}{\partial y} + \frac{\partial M_{xy}}{\partial x} - Q_y = I_2 \ddot{v}_0 + I_3(\ddot{\theta}_y) + I_4 \ddot{v}_0^* + I_5 \ddot{\theta}_y^*$$

$$\delta u_0^* : \frac{\partial N_x^*}{\partial x} + \frac{\partial N_{xy}^*}{\partial y} = I_3 \ddot{u}_0 + I_4(\ddot{\theta}_x) + I_5 \ddot{u}_0^* + I_6 \ddot{\theta}_x^*$$

$$\delta v_0^* : \frac{\partial N_y^*}{\partial y} + \frac{\partial N_{xy}^*}{\partial x} = I_3 \ddot{v}_0 + I_4(\ddot{\theta}_y) + I_5 \ddot{v}_0^* + I_6 \ddot{\theta}_y^*$$

$$\delta\theta_x^* : \frac{\partial M_x^*}{\partial x} + \frac{\partial M_{xy}^*}{\partial y} - Q_x^* = I_4 \ddot{u}_0 + I_5(\ddot{\theta}_x) + I_6 \ddot{u}_0^* + I_7 \ddot{\theta}_x^*$$

……(2.4.g)

## III. VIBRATION ANALYSIS OF FG-GRAPHENE PLATES USING HSDT

Composite rectangular plates are generally classified by referring to the type of support used. The analytical solutions of the above equations for simply supported FG-graphene plates are dealt here. Assuming that the plate is simply supported in such a manner that normal displacement is admissible, but the tangential displacement is not, solution functions that completely satisfy the boundary conditions in the equations below are assumed as:

$$u_0(x,y) = \sum_{m=1}^{\infty} \sum_{n=1}^{\infty} U_{mn} \cos\alpha x \sin\beta y$$

$$v_0(x,y)=\sum_{m=1}^{\infty}\sum_{n=1}^{\infty}V_{mn}\sin\alpha x\cos\beta y$$

$$w_0(x,y)=\sum_{m=1}^{\infty}\sum_{n=1}^{\infty}W_{mn}\sin\alpha x\sin\beta y$$

$$\theta_x(x,y)=\sum_{m=1}^{\infty}\sum_{n=1}^{\infty}X_{mn}\cos\alpha x\sin\beta y$$

$$\theta_y(x,y)=\sum_{m=1}^{\infty}\sum_{n=1}^{\infty}Y_{mn}\sin\alpha x\cos\beta y \qquad \text{..... (3.a)}$$

$$u_0^*(x,y)=\sum_{m=1}^{\infty}\sum_{n=1}^{\infty}U_{mn}^*\cos\alpha x\sin\beta y$$

$$v_o^*(x,y)=\sum_{m=1}^{\infty}\sum_{n=1}^{\infty}V_{mn}^*\sin\alpha x\cos\beta y$$

$$\theta_x^*(x,y)=\sum_{m=1}^{\infty}\sum_{n=1}^{\infty}X_{mn}^*\cos\alpha x\sin\beta y$$

$$\theta_y^*(x,y)=\sum_{m=1}^{\infty}\sum_{n=1}^{\infty}Y_{mn}^*\sin\alpha x\cos\beta y$$

for $\mathbf{0 \le x \le a ; 0 \le y \le b}$

The mechanical load is expanded in double Fourier sine series as:

$$q(x,y)=\sum_{m=1}^{\infty}\sum_{n=1}^{\infty}Q_{mn}\sin\alpha x\sin\beta y \qquad \text{..... (3.b)}$$

Where,

$\alpha=\frac{m\pi}{a}$ and $\beta=\frac{n\pi}{b}$ and *m* and *n* are modes numbers, and ω is the natural frequency of the system.

The natural frequencies and vibration modes for the plates by solving the Eigen value problem $([S]-\omega^2[M])X=0$, where X are the modes of vibration associated with the natural frequencies defined as ω.

## IV. RESULTS AND DISCUSSIONS

### *A. Comparative Study*

Validation of the present higher-order shear deformation theory in predicting the frequencies of a simply supported functionally graded GNP reinforced composite plates, examples are presented and discussed.

The polymer Epoxy is selected as the matrix. The material properties of which are:

$$E^m = 3\ GPa\ , \rho^m = 1.2\frac{g}{cm^3}, \vartheta^m = 0.34$$

GNP graphene nano platelets are taken as the reinforcements and its properties are:

$E_{GNP} = 1.01\ Tpa,$

$G_{GNP} = 0.42\ TPa,$

$\vartheta^{GNP} = 0.186$ and

$\rho^{GNP} = 1060\frac{kg}{m^3}.$

$l_{GNP}$ , $w_{GNP}$ and $h_{GNP}$ aZre the average length , width, and thickness of the GNP's and their values respectively 2.5µm,1.5µm,1.5nm.Effective material properties of the composite with 1% weight fraction of GNP is reinforced is

$E^c$=10.2892$GPa$,

$\upsilon_c$=0.338,and $\rho_c$=1.1984$\frac{g}{cm^3}$.

The GNP volume fractions at different weight fractions are caluculated and tabulated in Table.I

TABLE .I
Different Weight Fractions And Their Voume Fractions Of Gnp's

| Weight fraction$(g_{GNP})$% | Volume fraction $(V_{GNP})$% |
|---|---|
| 0.2 | 0.002264 |
| 0.6 | 0.006787 |
| 1 | 0.011314 |

Presently computed results for different values of Weight fraction and side-to-thickness ratios (*a*/*h*) are presented in Table II. For convenience, natural frequency ω has been non-dimensionalized as $\overline{\omega} = \omega h\sqrt{\rho_m/E_m}$.

From Table II, it can be observed that the values slightly lower than Mahhamad Arefi et al [2] in which FSDT theory was used for the analysis purpose. Where the HSDT approach gives accurate results than FSDT because of that we get lesser values than FSDT results.

TABLE .II
Comparison of non-dimensional natural frequency ($\overline{\omega} = \omega h\sqrt{\rho_m/E_m}$) subjected to Sinusoidal loading

| Weight Fraction $g_{GNP}$=1 | a/h = 10 | | a/h = 20 | |
|---|---|---|---|---|
| | Present | FSDT[2] | Present | FSDT[2] |
| UD | 0.12037 | 0.1216 | 0.1348 | 0.1378 |
| FG-X | 0.05894 | 0.06121 | 0.0734 | 0.0742 |

TABLE 5.3
Non-Dimensional Natural Frequency FG – GNP Composite Plate For Various Distributions At Different Side To Thickness Ratios Subjected To Sinusoidal Loading

| Side-to-thickness ratio | Type of Distribution | $g_{GNP}$=0.2 | $g_{GNP}$ = 0.6 | $g_{GNP}$= 1 |
|---|---|---|---|---|
| 10 | UD | 0.04012 | 0.069112 | 0.120378 |
| | FG-X | 0.005577 | 0.083634 | 0.1348048 |
| 20 | UD | 0.010514 | 0.02979 | 0.058944 |
| | FG-X | 0.011936 | 0.044312 | 0.0734661 |
| 50 | UD | 0.0042021 | 0.01278 | 0.023579 |
| | FG-X | 0.0056243 | 0.0135002 | 0.037801 |
| 100 | UD | 0.0021278 | 0.00604 | 0.011789 |
| | FG-X | 0.003504 | 0.007462 | 0.0131185 |

*B. Comparative study:*

The variation of Fundamental frequency with the change in side-to-thickness ratio and for different GNP distributions at various weight fractions are presented in Table .3. These results are plotted and compared with the standard values.

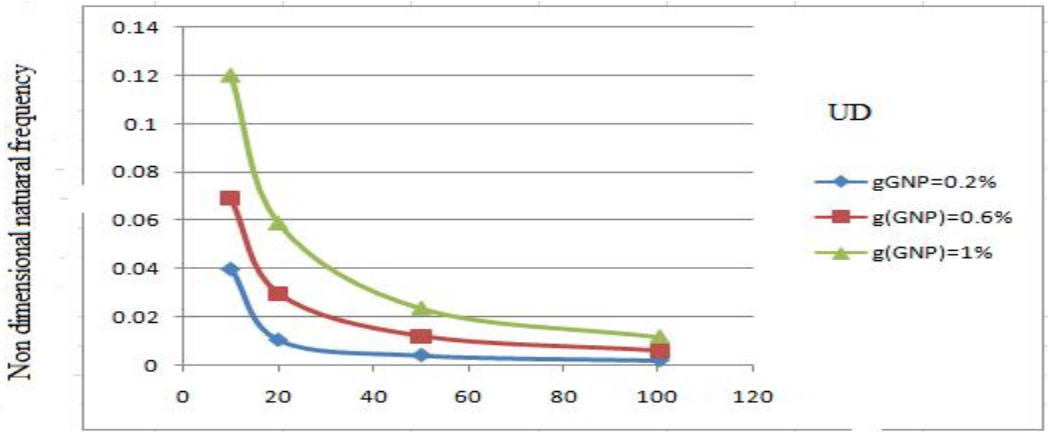


Figure. 3 Effect of side to thickness ratios on the non-dimensional natural frequency of UD plate at different weight fractions

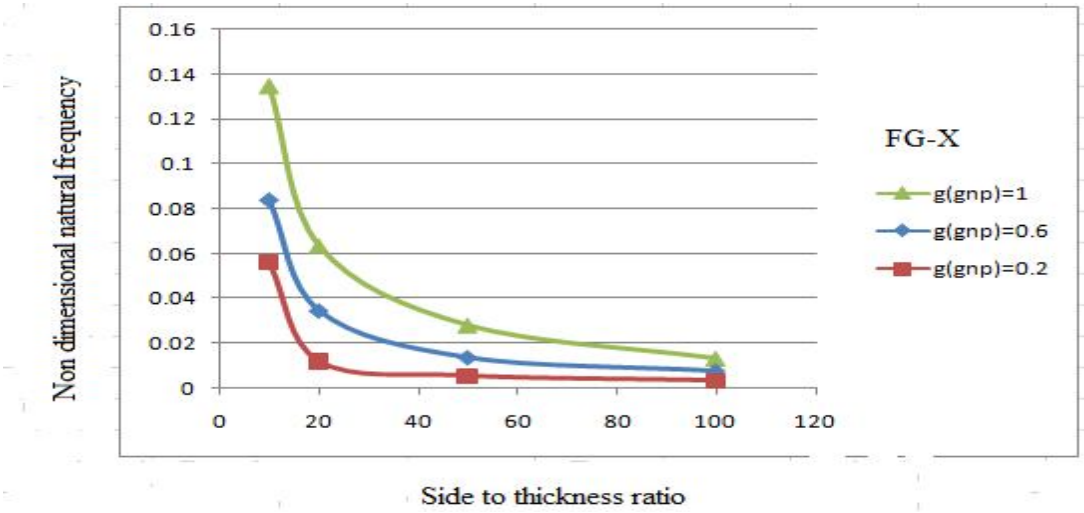


Figure.4 Effect of side to thickness ratios on the non-dimensional natural frequency of FG-X plate at different weight fractions

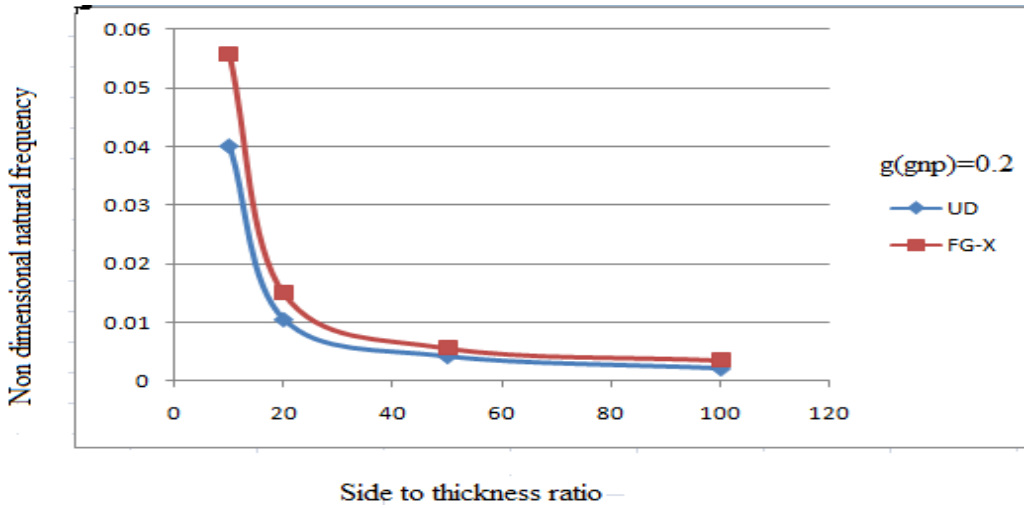


Figure.5 Comparison of non-dimensional natural frequency of FG-GNP plate for different distributions at $g_{GNP} = 0.2$

*ISSN: 2321-9653; IC Value: 45.98; SJ Impact Factor: 7.177*
*Volume 7 Issue VII, July 2019- Available at www.ijraset.com*

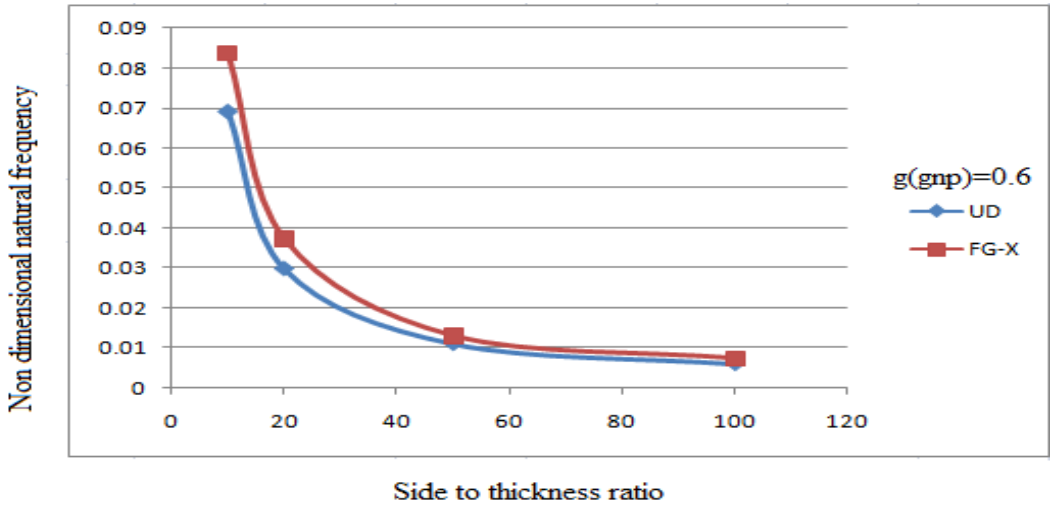


Figure.6 Comparison of non-dimensional natural frequency of FG-GNP plate for different distributions at $g_{GNP} = 0.6$

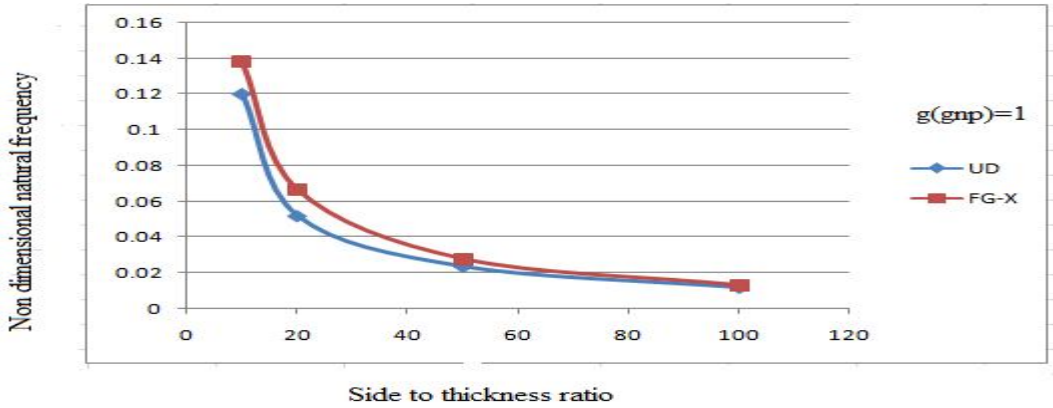


Figure.7 Comparison of non-dimensional natural frequency of FG-GNP plate for different distributions of FG-GNP plate for different distributions at $g_{GNP} = 1$

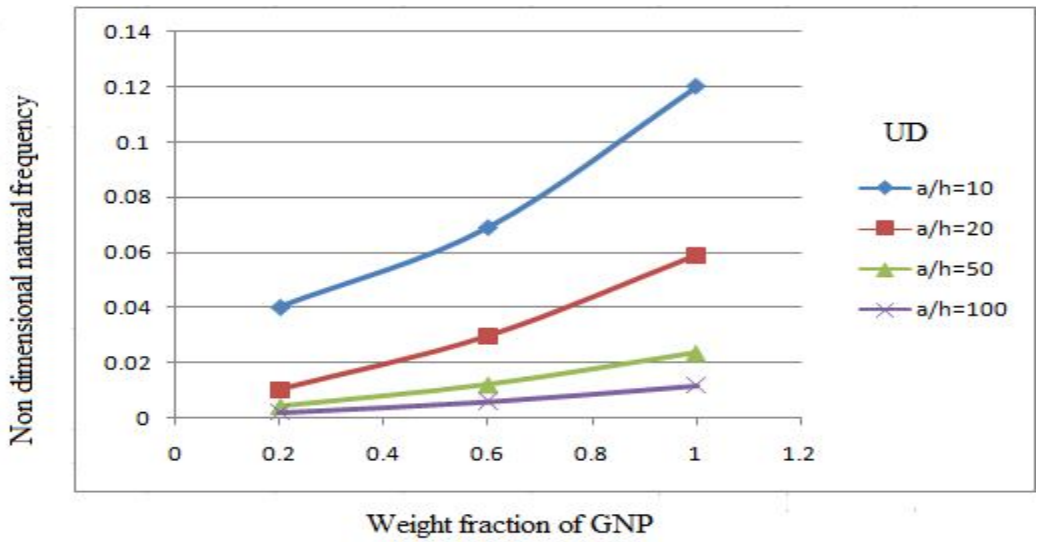


Figure.8 Effect of volume fractions on the non-dimensional natural frequency of a uniformly distributed FG-GNP plate for different values of a/h ratios

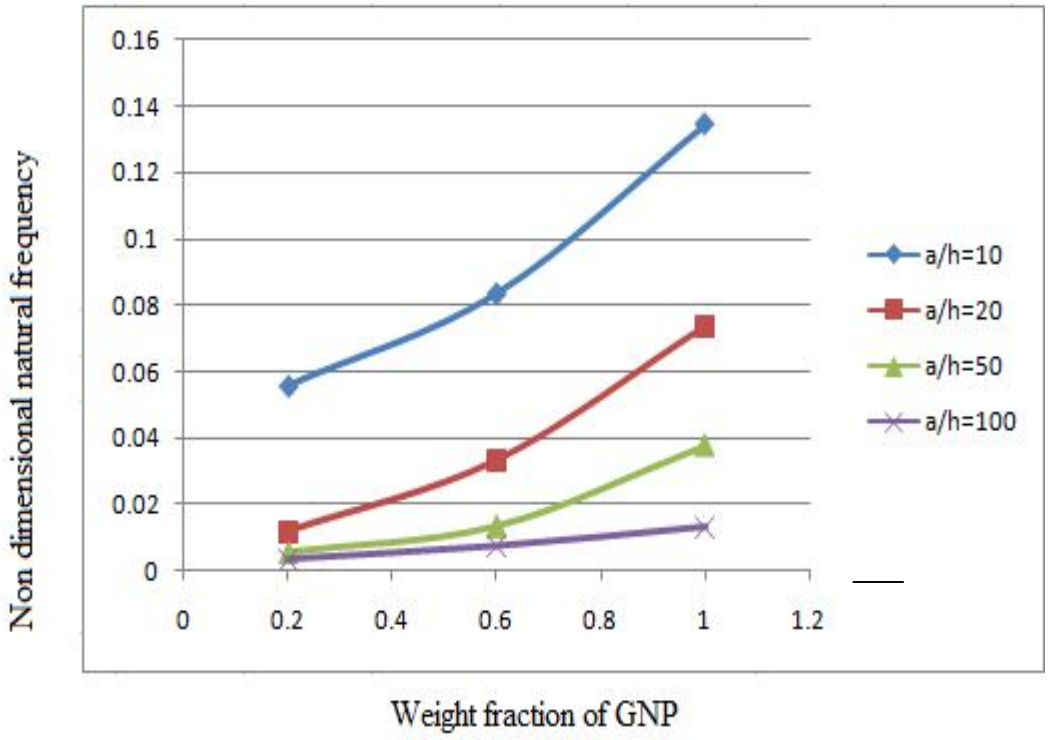


Figure.9 Effect of volume fractions on the non-dimensional natural frequency of a FG-X plate for different values of a/h ratios

Fig.3 and Fig.4 shows the variation of the non-dimensional natural frequency with respect to side-to-thickness ratios (*a*/*h*) for various distributions of GNP, according to present higher-order shear deformation theory. From this, it is clear that the effect of decreasing frequencies is felt with the increase in a/h ratio for simply supported boundary conditions. The effect of shear deformation decreases with the increasing values of *a*/*h* and decreasing values of weight fraction Figure.5 Figure.6 and Figure.7 shows the comparison of $\overline{\omega}$ of FG-GNP plate for different distributions at various weight fractions of GNP. It is clear from these graphs that X-distribution is more effective than the uniform distribution of as the variation of $\overline{\omega}$ is consistent for FG-X.

In Figure.8 and Figure.9, it is observed that as the a/h ratio increases the value of fundamental frequency decreases and with the increase in weight fraction of GNP for a particular a/h ratio, the value of fundamental frequency increases. It is also proven from the graph that the effect of side-to-thickness ratio increases the change in fundamental frequency. That is, the rate of change in fundamental frequency increases when we go to the higher values of a/h values.

## V. CONCLUSIONS

Analytical formulations and solutions for free vibration characteristics of FG-GNP reinforced composite plates is developed using the higher-order shear deformation theory , which account for transverse extensibility and without enforcing zero shear on the top and bottom of the FG-GNP plates. Hamilton's principle is used in deriving the equations of motion. Closed form solutions are derived for simply supported boundary conditions using Navier's method and solving the Eigen value problem. The accuracy and efficiency of the present theory have been presented in the results and discussions of the FG-GNP plates. From the results it is proven that with the increase in weight fractions, the fundamental frequency increases and also it is observed that as the side to thickness ratio increases the fundamental frequency decreases.It is also observed that the natural frequency of FG-X plate are greater than that UD plate. Hence, the present results which are obtained using this theory can be used as reference for further studies. From the above, it is concluded that the proposed theory is simple and accurate in analyzing the free vibration behavior of FG-GNP composite plates.

## REFERENCES

[1] Mitao song, Sritawat Kitipornchai, Jie Yang (2016) Free and forced vibrations of functionally graded polymer composite plates reinforced with graphene nano platelets.
[2] Mohammad Arefi, Elyas Mohammad-RezaeiBidgoli (2018)Free vibrations of FG polymer composite reinforced with graphene nano platelets.
[3] Adam Mrozek, TadeuszBurczynsk Examination of mechanical properties of graphene allotropes by means of computer stimulation.
[4] Zhonghua Ni, Hao Bu, Min Zou, Hong Yi, Kedonj Bi Anisotropic mechanical properties of graphene sheets from molecular dynamics.
[5] ND Phan, JN Reddy 2201-2219,1985 Analysis of laminated composite plates using higher order shear deformation theory.
[6] HT Thai, Seung-Eock Kim 626-633,2010 Free vibration of laminated composite plates using two variable refined plate theory.
[7] Jie Yang, Da Che, SritawatKitipornchai Buckling and free vibration analysis of functionally graded graphene reinforced porous nano composite plates based on chebyyshew-Ritz method.
[8] Chuang Feng, Sritawat Kitipornchai,Jie Yang(2017) Non linear free vibrations of functionally graded composite beams reinforced with graphenenano platelets(GPLS) .
[9] SritawatKitipornchai, D Chen,J Yang –Materias and design ,2017Functionally graded porous beams reinforced by graphene platelets.
[10] Zhang, L.W., Song, Z.G., Liew, K.M.,(2015) State-space Levy method for vibration analysis of FG-CNT composite plates subjected to in-plane loads based on higher-order shear deformation theory, Composite Structures.
[11] BabakSafaei, Fatta Hi Free vibrational response of single layered graphene embedded in an elastic matrix using different plate models.
[12] Aiwen Wang, Weizhang Vibration and bending behaviour of FG nano composite doubly curved shallow shells reinforced by graphenenano platelets.
[13] T.Kant, K.Swaminathan, Analytical solutions for free vibration of laminated composite and sandwich plates based on a higher-order refined theory, Composite Structures 53 (2001) 73-85.
[14] Yue L, Pircheragi G, Monemian SA,Manas-zloczower I. Epoxy composites with carbon nanotubes and graphene nano platelets-Dispersion and synergy effects. Carbon N Y2014;78:268-278
[15] Wu H, Yang J,Kitiporchai S. Dynamic instability of functionally graded multilayer graphene nano composite beams in thermal environment. Compos struct 2014;162:244-254.
[16] Wang Y ,Feng C, Zhao Z, Yang J .Buckling of graphene platelet reinforced composite cylindrical shells with cut out .Int J Struct Stab Dyn 2018 .
[17] Rafiee MA, Rafiee J, Wang Z , Song H, Yu Z-Z koratkar N. Enhanced mechanical properties of nano composite at lo graphene content .ACS Nano 2009;3(12):3884 – 3890
[18] Xiao Huang , Zongyou yin , Shixin Wu, Xiaoying Qiyuan He , Qichun Zhang, Qingyu Yan , Freddy Boey, and Hua Zhang Graphene – Based Materials : Synthesis ,characterization ,properties, and Applications.
[19] Sasha Stankovich, Dmitriy A, Dikin, Geoffrey H, B.Dommett, Kevin M. Kohlhass , Eric J.Zimney, Eric stach , Richaed D. Piner ,SonBinh T. nguyen & Rodney S. Ruoff. Graphene –based composite Materials.
[20] Mohammed A. Rafiee, Javad Rafiee, Zhou Wang , Huaihe Song , Zhong –Zhen Yu, and Nikhil Koratkar. Enahanced Mechanical Properties of Nano composites at Low Graphene content.

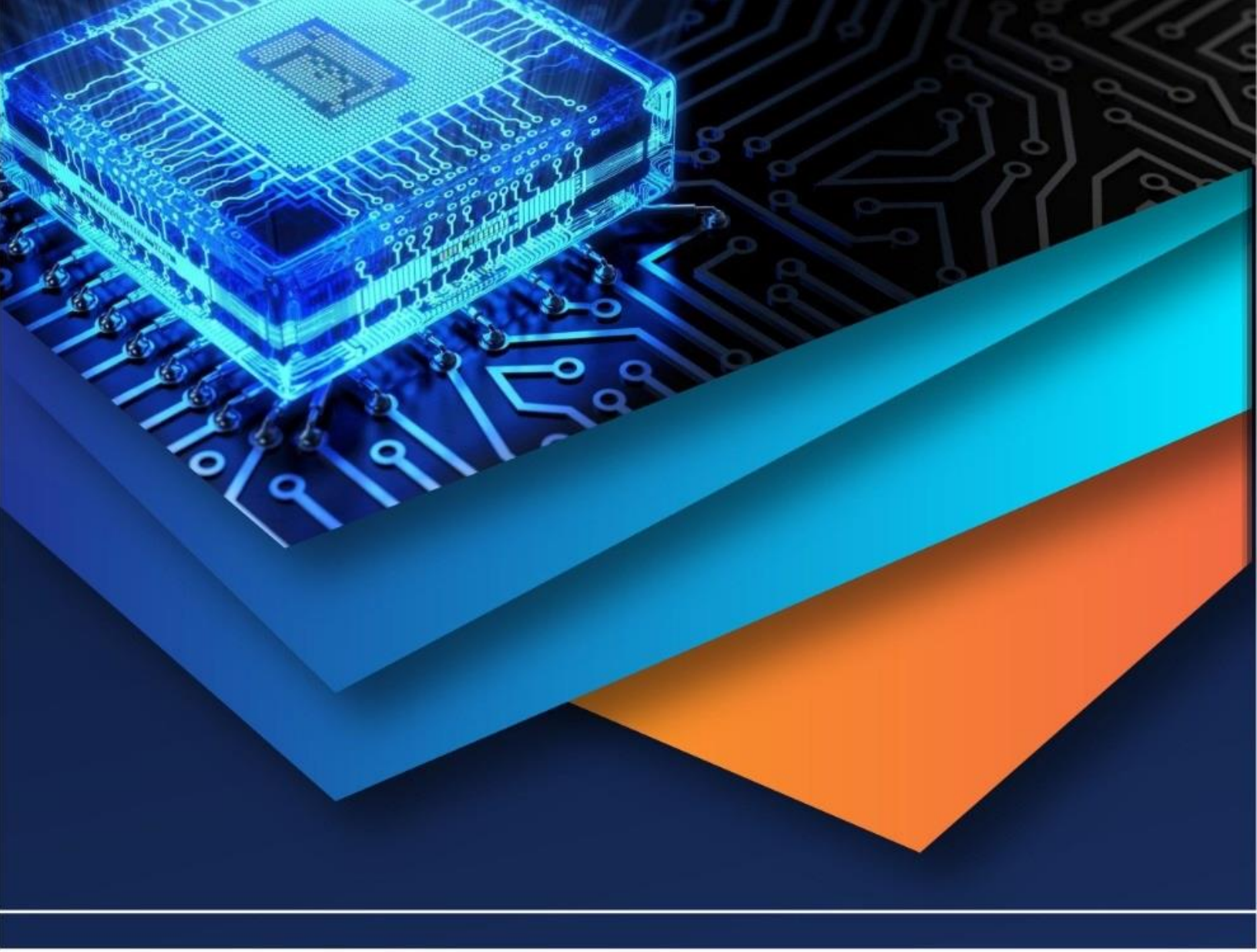

10.22214/IJRASET

45.98

IMPACT FACTOR: 7.129

IMPACT FACTOR: 7.429

# INTERNATIONAL JOURNAL FOR RESEARCH

IN APPLIED SCIENCE & ENGINEERING TECHNOLOGY